

Article

Loliolide from *Artemisia princeps* Suppresses Adipogenesis in Human Bone Marrow-Derived Mesenchymal Stromal Cells via Activation of AMPK and Wnt/ β -catenin Pathways

Jung Hwan Oh ¹, Fatih Karadeniz ¹, Mi-Soon Jang ², Hojun Kim ³, Youngwan Seo ³ and Chang-Suk Kong ^{1,4,*} 

¹ Marine Biotechnology Center for Pharmaceuticals and Foods, College of Medical and Life Sciences, Silla University, Busan 46958, Korea; wjdghks0171@naver.com (J.H.O.); karadenizf@outlook.com (F.K.)

² Food Safety and Processing Research Division, National Institute of Fisheries Science, Busan 46083, Korea; suni1@korea.kr

³ Division of Marine Bioscience, Korea Maritime and Ocean University, Busan 49112, Korea; tearhkim@gmail.com (H.K.); ywseo@kmou.ac.kr (Y.S.)

⁴ Department of Food and Nutrition, College of Medical and Life Sciences, Silla University, Busan 46958, Korea

* Correspondence: cskong@silla.ac.kr; Tel.: +82-51-999-5429

Featured Application: Loliolide has potential to be used as a functional food ingredient with anti-obesity properties.

Abstract: Regulating the adipogenic differentiation mechanism is a valid and promising mechanism to battle obesity. Natural products, especially phytochemicals as nutraceuticals, are important lead molecules with significant activities against obesity. Loliolide is a monoterpenoid hydroxyl lactone found in many dietary plants. The effect of loliolide on adipogenic differentiation is yet to be determined. Therefore, the present study aimed to evaluate its anti-adipogenic potential using human bone marrow-derived mesenchymal stromal cells (hBM-MSCs) and assess its mechanism of action. Adipo-induced hBM-MSCs were treated with or without loliolide and their adipogenic characteristics were examined. Loliolide treatment decreased the lipid accumulation and expression of adipogenic transcription factors, PPAR γ , C/EBP α , and SREBP1c. Adipo-induced hBM-MSCs also displayed increased AMPK phosphorylation and suppressed MAPK activation following loliolide treatment according to immunoblotting results. Importantly, loliolide could stimulate Wnt10b expression and active β -catenin translocation to exert PPAR γ -linked adipogenesis suppression. In conclusion, loliolide was suggested to be a potential anti-adipogenic agent which may be utilized as a lead compound for obesity treatment or prevention.

Keywords: adipogenesis; AMPK; *Artemisia princeps*; hBM-MSC; loliolide; β -catenin



Citation: Oh, J.H.; Karadeniz, F.; Jang, M.-S.; Kim, H.; Seo, Y.; Kong, C.-S. Loliolide from *Artemisia princeps* Suppresses Adipogenesis in Human Bone Marrow-Derived Mesenchymal Stromal Cells via Activation of AMPK and Wnt/ β -catenin Pathways. *Appl. Sci.* **2021**, *11*, 5435. <https://doi.org/10.3390/app11125435>

Academic Editor: Monica Gallo

Received: 3 May 2021

Accepted: 9 June 2021

Published: 11 June 2021

Publisher's Note: MDPI stays neutral with regard to jurisdictional claims in published maps and institutional affiliations.



Copyright: © 2021 by the authors. Licensee MDPI, Basel, Switzerland. This article is an open access article distributed under the terms and conditions of the Creative Commons Attribution (CC BY) license (<https://creativecommons.org/licenses/by/4.0/>).

1. Introduction

Obesity is a serious medical concern in today's world and characterized by excess fat accumulation which is not only an aesthetic problem but also an underlying cause of several diseases such as cardiovascular diseases, different types of cancer, organ failures, and diabetes [1,2]. Excess accumulation of body fat occurs through elevated levels of adipose tissue formation, which is a result of adipogenic differentiation of adipogenic progenitor stem cells. However, recent studies clearly showed that adipose tissue, and adipogenesis thereof, is not only linked to obesity but also several other diseases [3,4]. The close and complex regulatory relations between white and brown adipose tissues, which are the most abundant distinct adipose tissues in the human body, are considered to be the reason behind the obesity onset and progression [4]. Adipose tissue consists of distinct tissues in addition to white and brown adipose tissues, such as bone-marrow adipose tissue. The differentiation capabilities and roles they take in various mechanisms in homeostasis make human mesenchymal stem cells promising targets for regenerative

medicine and have been utilized in several studies against diabetes, cardiovascular diseases, and osteoarthritis [5].

The differential tendencies towards adipogenesis in progenitor cells occurs not only in adipose tissue but in other parts of the body as well where mesenchymal stromal cells are present. For example, osteoporosis is a very common bone disorder where bone-marrow cells tend to differentiate into adipocytes rather than osteoblasts under the influence of several effectors including obesity [6]. In bone tissue, activation of the intracellular mechanisms that lead to stimulation of adipogenic differentiation elevates the adipocyte count and deteriorates the balance between bone formation and bone adipose tissue [7]. In addition, studies showed that differentiation of stromal cells in one part of the body affects the other progenitor cells. For instance, increased adipogenic differentiation of bone-marrow stromal cells induce changes in overall body adiposity through elevated adipogenesis in adipose tissue progenitor cells [8,9]. Mesenchymal stem cells are one of the widely studied in vitro models for studies targeting differential regulation of adipogenic progenitor cells to develop novel strategies against obesity and osteoporosis as well as developing regenerative medicine [4].

Peroxisome proliferator-activated receptor (PPAR) γ is the main regulatory protein responsible for the onset of adipogenesis [10]. Several other upstream and downstream effectors of PPAR γ are involved in the stimulation of adipogenic differentiation and adipocyte maturation of MSCs. These effectors include SREBP1 and C/EBP α [10,11]. On the other hand, Wnt/ β -catenin signaling, the activation of which is vital for osteogenic differentiation, is suppressed during adipogenesis in order to tilt MSC differentiation balance towards adipogenesis [12]. Recently, several studies focused on regulation of MSC differentiation: inhibiting the adipogenesis while enhancing osteoblastogenesis to prevent or treat obesity-linked complications [13,14]. There are studies addressing obesity using MSCs derived from adipose tissue [5]. However, utilizing hBM-MSCs in order to regulate adipogenesis in relation to osteoblastogenesis is another aspect of the obesity-linked osteoporosis which was aimed to be achieved by the current study.

Loliolide is a common monoterpene hydroxyl lactone mainly found in algae, although it is ubiquitously present in other plants as an allelochemical response modulator for plant-to-plant interactions [15]. Studies reported bioactive properties for loliolide such as antioxidant, antiviral, anticancer and hair promoting activities [16,17]. Loliolide has been shown to inhibit adipogenic differentiation of 3T3-L1 murine pre-adipocytes [18] and decrease the adiposity of liver in high-fat diet in vivo models [19]. However, to the best of our knowledge, its effects on the adipogenic differentiation of MSCs have not reported yet. To promote loliolide as a lead compound against obesity and obesity-linked complications, its ability to hinder adipogenesis through mechanisms linked to other differentiation mechanisms must be elucidated. In this context, the present study aimed to evaluate the anti-adipogenic properties of (-)- loliolide, isolated from *Artemisia princeps*, in adipo-induced hBM-MSCs to conclude whether it is able to block the adipogenesis in bone-marrow adipose tissue. Current findings may also serve as a reference for future studies utilizing loliolide in other MSCs such as white and brown adipose tissue derived MSCs.

2. Materials and Methods

2.1. Loliolide

Loliolide was isolated from *A. princeps* as reported by Kim [20]. Identification and characterization were carried out via comparison of NMR data with the published literature [21].

2.2. hBM-MSC Culture and Adipogenesis

The cells used in this study were purchased from PromoCell (C-12974, Heidelberg, Germany). Unless otherwise noted, 6-well plates were used to seed and proliferate the hBM-MSCs (1×10^6 cells/well) and cells were fed Mesenchymal Stem Cell Growth Medium (C-28009, PromoCell). Cultured cells were kept in 37 °C incubators and the CO₂ levels were set at 5%. The hBM-MSCs were induced for adipogenesis by exchanging the cul-

ture medium of confluent cells with Mesenchymal Stem Cell Adipogenic Differentiation Medium 2 (C-28016, PromoCell). Differentiation was continued by feeding the cells with fresh differentiation medium every third day until the time of the experiment. The cells were treated with loliolide during the first introduction of differentiation medium only and the subsequent medium changes did not include loliolide treatment.

2.3. MTT Assay for Cell Viability

Prior to experiments, cytotoxicity of loliolide in hBM-MSCs was assessed by MTT assay. Briefly, cells were seeded in 96-well plates (1×10^3 cell/well) and incubated for 24 h. Next, the cells were treated with varying concentrations of loliolide (1, 5, 10, and 25 μM). Following loliolide treatment, the wells were aspirated and 100 μL of 1 mg/mL MTT working solution (in distilled water) was added and the plates were incubated for 4 h. After 4 h, the reaction was stopped by adding 100 μL 100% DMSO. Finally, the absorbance was observed at 540 nm with a MultiSkan GO microplate reader (Thermo Fisher Scientific, Waltham, MA, USA). The viability of hBM-MSCs were calculated as a relative percentage of the untreated control cells.

2.4. Staining of Intracellular Lipid Accumulation

Triglyceride droplets in hBM-MSCs as a differentiation marker was examined by staining intracellular lipid droplets with Oil Red O. At Day 10 of adipogenesis inducement, differentiated hBM-MSCs in 6-well plates were fixed by adding 10% formaldehyde to the aspirated wells and keeping the plates in room temperature for 1 h. After 1 h, 1 mL of 0.5% Oil Red O staining solution (*wt/v*, in 3 parts isopropanol and 2 parts distilled water) was added to each well after the medium was removed from the wells. The plates were kept at room temperature for another 1 h. The Oil Red O staining solution was removed from wells after 1 h and the plates were air-dried. One milliliter of PBS was added to wells prior to staining and images were taken by a microscope (Olympus, Tokyo, Japan). Next, the wells were aspirated, and the stain was eluted from the lipid droplets via addition of 100% isopropanol. Quantification of the eluted stain amount as a representative of lipid accumulation was performed using the optical density of the wells at 500 nm with a MultiSkan GO microplate reader (Thermo Fisher Scientific, Waltham, MA, USA). The final optical density values were normalized with total protein concentrations.

2.5. Quantitative Reverse Transcription PCR

The hBM-MSCs were differentiated into mature adipocytes as described above. Total RNA was extracted from differentiated (loliolide-treated and non-treated) and non-differentiated hBM-MSCs with a commercial RNA extraction kit (AccuPrep Universal; Bioneer, Daejeon, Korea). The cDNA was synthesized using equal amounts (2 μg) of total RNA from each group. A commercial master-mix was used for the cDNA synthesis (Cell Script All-in-One cDNA Synthesis Master Mix; CellSafe, Yongin, Korea). Reaction was carried out according to protocol provided by the manufacturer with the following temperature settings in a T100 thermocycler (Bio-Rad Laboratories, Inc., Hercules, CA, USA): 42 $^{\circ}\text{C}$ for 60 min and 72 $^{\circ}\text{C}$ for 5 min. Next, real time PCR analysis was completed in TP800 Thermal Cycler DiceTM Real Time System (Takara Bio, Ohtsu, Japan). The qPCR was carried out via commercial qPCR kit (Luna[®] Universal qPCR Mix, New England Biolabs, Ipswich, MA, USA) with the primers described earlier [22]. The reaction was performed for 30 cycles consisting of three steps: 95 $^{\circ}\text{C}$ for 45 s, 60 $^{\circ}\text{C}$ for 1 min, and 72 $^{\circ}\text{C}$ for 45 s. The amplifications of target genes were calculated as relative fold change compared to the differentiated but not loliolide-treated group. All expression levels were normalized against the reference gene, β -actin.

2.6. Western Blot Analysis

To detect the protein levels in differentiated hBM-MSC adipocytes, standard Western blot analysis was conducted. At Day 10 after the adipogenesis inducement, the hBM-MSCs

in 6-well plates were homogenized using ice-cold RIPA buffer via vigorous pipetting. The lysates were then transferred into tubes and centrifuged ($13,000\times g$) at $4\text{ }^{\circ}\text{C}$ for 15 min. The supernatants were used for protein detection. In the case of nuclear fractions, the nuclear total protein was extracted using a commercial kit (NE-PERTM nuclear extraction kit; #78835; Thermo Fisher Scientific, Waltham, MA, USA) following the protocol provided by the manufacturer. Total protein contents of the samples were analyzed using a BCA protein assay kit (Thermo Fisher Scientific, Waltham, MA, USA) following the manufacturer's protocol. The supernatants containing equal amounts (20 μg) of protein were separated by sodium dodecyl sulfate–polyacrylamide gel electrophoresis (4% stacking and 10% separating gels). Separation was followed by the transfer of proteins to polyvinylidene fluoride membranes (Amersham Bioscience, Westborough, MA, USA) from gels. Next, the membranes were blocked for 1 h at room temperature. Five percent skim milk (*v/v*) prepared with TBS-T buffer was used to block the membranes prior to hybridization overnight at $4\text{ }^{\circ}\text{C}$ with primary antibodies against tested proteins: PPAR γ (#2443; Cell Signaling Technology, Danvers, MA, USA), CCAAT/enhancer-binding protein (C/EBP) α (#2295; Cell Signaling Technology), sterol regulatory element-binding protein 1c (SREBP1c) (ab3259; Abcam, Cambridge, England, UK), p38 (#8690; Cell Signaling Technology), phospho(p)-p38 (#4511; Cell Signaling Technology), JNK (LF-PA0047; Thermo Fisher Scientific, Waltham, MA, USA), p-JNK (sc-293136; Santa Cruz Biotechnology, Santa Cruz, CA, USA), ERK (#4695; Cell Signaling Technology), p-ERK (#4370; Cell Signaling Technology), AMPK (#2603; Cell Signaling Technology), p-AMPK (#2531; Cell Signaling Technology), and β -actin (sc-47778; Santa Cruz Biotechnology). Hybridized proteins were then stained at room temperature for 2 h with horseradish peroxidase-conjugated secondary antibodies specific to hybridizing antibody organism. Stained proteins were then detected using an ECL kit (Amersham Bioscience). The images of the bands on the membrane after ECL kit-treatment were obtained with a Western blot imaging system (CAS-400SM; Davinch-K, Seoul, Korea).

2.7. Immunofluorescence Staining

The intracellular perilipin-1, PPAR γ , and Wnt 10b protein expressions were visualized by immunofluorescence staining. The hBM-MSCs were grown and induced to differentiate on glass coverslips placed in 6-well plates. The fluorescence staining was carried out on Day 10 of differentiation. The fixation, washing, and permeabilization of the cells were performed using the solutions and the protocol provided by Immunofluorescence Application Solutions Kit (#12727; Cell Signaling Technology). Alexa Fluor 488 (A-11008; Invitrogen)-conjugated anti-perilipin-1 (ab3526; Abcam) and anti-PPAR γ (ab9256; Abcam) antibodies were used to stain target proteins. For the normalization and confirmation, viable cells were also stained with DAPI (#8961; Cell Signaling Technology) containing ProLong Gold Antifade reagent. Images of the stained adipocytes were taken using an Olympus fluorescence microscope equipped with a digital camera and processed with the Multi-Gauge software.

2.8. Statistical Analysis

All results are given as \pm SD ($n = 3$) where applicable. The statistical difference between sample treatment groups was determined using one-way analysis of variance (ANOVA) coupled with post-hoc Duncan's multiple range test using SAS (v9.1) software (SAS Institute, Cary, NC, USA). Meaningful statistical difference was defined at $p < 0.05$ level.

3. Results

3.1. Lipid Accumulation by Differentiated hBM-MSCs

Prior to assessing its anti-adipogenic properties, the cytotoxicity of loliolide was tested on hBM-MSCs via MTT assay. The results show that, with up to 10 μM loliolide treatment, there was no loss of viability (Figure 1B). The first significant decrease in viable cell amount was at 25 μM . Therefore, further loliolide treatment was carried out using 10 μM as the highest concentration. Adipogenesis of hBM-MSCs in response to loliolide treatment

following adipogenic differentiation medium administration was evaluated at Day 10 of differentiation. Maturation of adipo-induced cells into adipocytes was confirmed by the lipid accumulation as intracellular lipid droplets. Most of the adipo-induced hBM-MSCs had lipid droplets displayed by positive Oil Red O stain compared to non-differentiated group (Figure 1C). Loliolide decreased the lipid accumulation dose-dependently starting at 5 μM concentration. Inhibitory effect of loliolide in intracellular triglyceride droplet levels was further confirmed by the quantification of Oil Red O stain. Loliolide-treated adipocytes displayed 8.86% and 29.88% less lipid accumulation, at 5 and 10 μM treatment, respectively, relative to the untreated control. Adipogenesis-induced accumulation of intracellular fat was also examined by fluorescence staining of the perilipin in adipocytes. Perilipin is a coating protein that bounds to the intracellular lipid droplets and has critical roles during adipogenesis. Perilipin expression in MSCs was reported to be upregulated during adipogenesis [23].

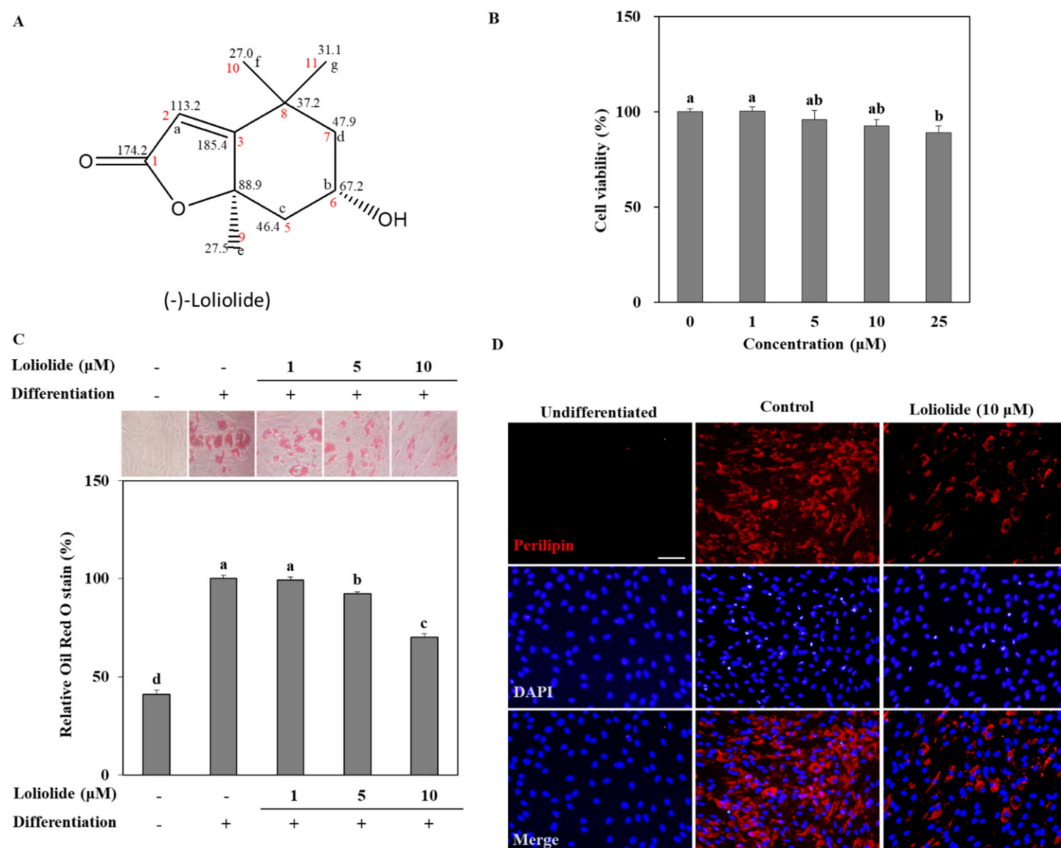


Figure 1. The effect of loliolide on intracellular triglyceride accumulation in adipo-induced hBM-MSCs. (A) Chemical structure of loliolide. (B) The effect of loliolide treatment on the hBM-MSC viability after 24 h assessed by MTT assay. Viability of the hBM-MSCs were given as a relative percentage of loliolide-untreated group. Different letters (a–e) above the sample groups indicate that the difference between each group is statistically significant ($p < 0.05$) compared to the untreated differentiated control. (C) The hBM-MSCs were differentiated into adipocytes in six-well plates with or without loliolide treatment (1, 5, and 10 μM). One group was left untreated and non-differentiated as the negative control. At Day 10 differentiation, intracellular triglyceride stores of mature adipocytes and non-differentiated hBM-MSCs were stained with Oil Red O. The triglyceride levels stored inside adipocytes were quantified as the amount of retained Oil Red O which was calculated via colorimetric measurement. Numerical data are $\pm\text{SD}$ ($n = 3$). Different letters (a–d) above the sample groups indicate that the difference between each group is statistically significant ($p < 0.05$) compared to the untreated differentiated control. (D) Images of fluorescence stained hBM-MSCs at incubation Day 10 after adipogenesis inducement (except undifferentiated untreated group which was fed growth medium only), stained with FITC conjugated anti-perilipin-1 antibody (red) and DAPI (blue) to highlight the nuclei. Scale bar, 100 μm .

As shown in Figure 1D, hBM-MSC adipocytes displayed over-expression of perilipin at Day 10 of differentiation. However, loliolide treatment (10 μ M) significantly inhibited perilipin expression, hence resulting in suppressed lipid accumulation.

3.2. The mRNA and Protein Levels of Adipogenic Markers during Adipogenic Differentiation of hBM-MSCs

The mRNA and protein levels of key adipogenic markers PPAR γ , C/EBP α , and SREBP1c were determined in hBM-MSC adipocytes. Adipogenic inducement of the hBM-MSCs increased the levels of PPAR γ , C/EBP α , and SREBP1c. Treatment with 10 μ M loliolide decreased mRNA and protein expression of all tested genes compared to untreated adipocytes (Figure 2A,B). Loliolide treated hBM-MSCs expressed 64.9%, 31.3%, and 73.2% less mRNA of genes PPAR γ , C/EBP α , and SREBP1c, respectively, compared to the untreated control (Figure 2A). Treatment with loliolide also led to significant decrease in the protein levels of PPAR γ and C/EBP α along with a slightly inhibited level of SREBP1c (Figure 2B). The effect of loliolide on PPAR γ signaling was also determined by fluorescence staining of the PPAR γ protein. The hBM-MSC adipocytes expressed high levels of PPAR γ accumulated in the nucleus relative to DAPI staining (Figure 2C). Loliolide significantly decreased the PPAR γ amount indicating, that it inhibited adipogenic differentiation of hBM-MSCs via suppressed PPAR γ activation.

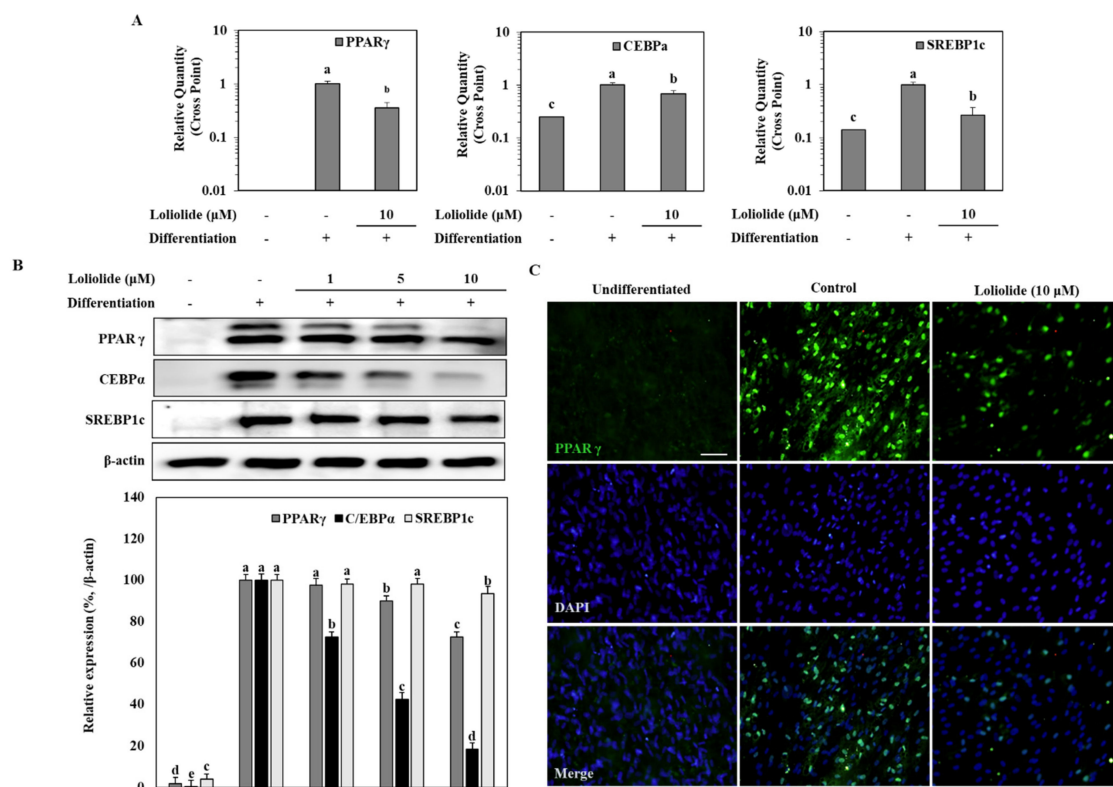


Figure 2. The effect of loliolide treatment on the mRNA and protein levels of adipogenic markers, PPAR γ , C/EBP α , and SREBP1c in hBM-MSC adipocytes. The hBM-MSCs were differentiated into adipocytes with or without loliolide treatment. One group was left untreated and non-differentiated as the negative control. PPAR γ , C/EBP α , and SREBP1c mRNA (A) and protein (B) expression levels were analyzed by RT-qPCR and Western blotting, respectively, at Day 10 of differentiation. β -actin was used as housekeeping gene and protein. Different letters (a–e) above the sample groups indicate that the difference between each group is statistically significant ($p < 0.05$) compared to the untreated differentiated control. (C) Images of fluorescence stained hBM-MSCs at incubation Day 10 after adipogenesis inducement (except undifferentiated untreated group which was fed growth medium only), stained with anti-PPAR γ antibody (green) and DAPI (blue). Scale bar, 100 μ m.

3.3. Activation of MAPK and AMPK Signaling Pathway during Adipogenic Differentiation of hBM-MSCs

The regulation of MAPK and AMPK signaling pathways are needed during the early stages of MSC adipogenesis. Activation of MAPKs is observed during adipogenesis to increase the adipogenic gene expression, while AMPK activation was shown to be suppressed as AMPK activation induces lipolysis, energy expenditure, and decrease in white adipose tissue [24,25]. Therefore, these pathways were examined in adipo-induced hBM-MSCs to underly the mechanism behind the anti-adipogenic effect of loliolide. To this end, phosphorylation levels of p38, ERK, and JNK was evaluated by Western blot. The levels of total MAPK expression were not altered with differentiation, while phosphorylation of these MAPKs was notably increased with adipogenesis (Figure 3A). Treatment with loliolide significantly decreased the adipogenesis-induced levels of phosphorylated (p-) p38 and JNK, whereas p-ERK levels were not affected. Next, activation levels of AMPK with or without an AMPK inhibitor (compound C) were analyzed by Western blot. The level of p-AMPK was inhibited by adipogenesis; however, loliolide treatment (10 μ M) significantly elevated the phosphorylation of AMPK, while total protein levels of AMPK were not changed in adipo-induced hBM-MSCs (Figure 3B). Further support for the effect of loliolide on AMPK phosphorylation was obtained from experiments using compound C (a known AMPK inhibitor) treatment along with loliolide. The compound C-only treated group displayed nearly diminished AMPK levels in adipo-induced hBM-MSCs as early as 6 h after administration of adipogenic differentiation medium. Loliolide treatment reverted the inhibitory effect of compound C on AMPK phosphorylation in a time-dependent manner (Figure 3C). Twelve hours after adipogenic inducement, loliolide treatment almost completely reinstated the phosphorylated AMPK levels despite the presence of compound C. These results indicate the involvement of MAPK/AMPK phosphorylation in loliolide-mediated suppression of adipogenesis.

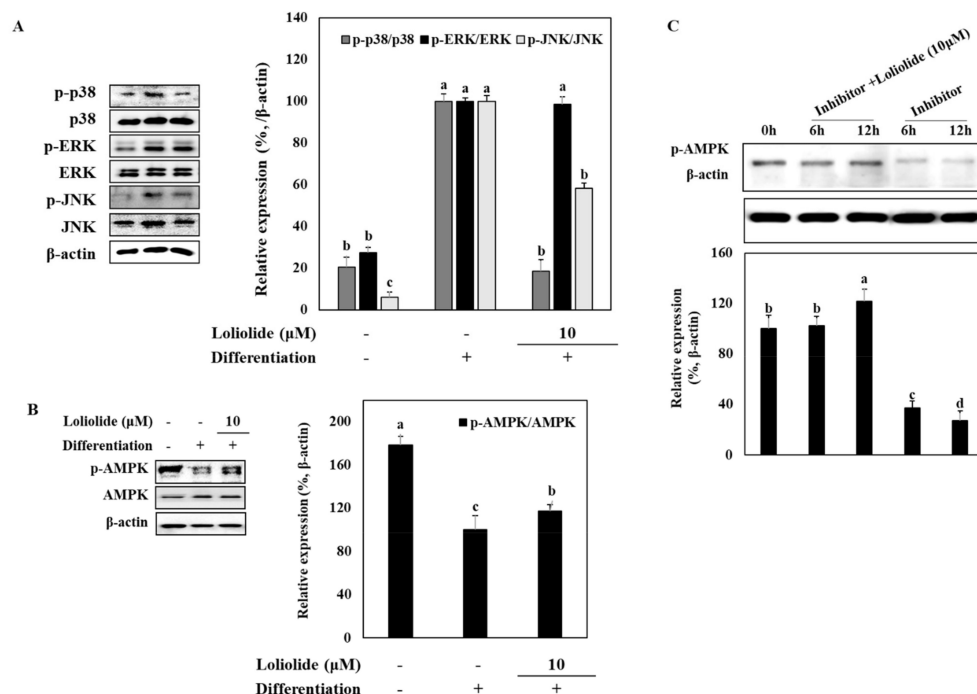


Figure 3. The effect of loliolide treatment on the protein and phosphorylation levels of p38, ERK, and JNK MAPKs and AMPK pathways. The hBM-MSCs were differentiated into adipocytes in six-well plates with or without loliolide treatment (10 μ M). One group was left untreated and non-differentiated as the negative control. The hBM-MSCs at Day 10 of differentiation were used for the analysis of total and phosphorylated (p-) MAPK and AMPK levels, namely p38, ERK, JNK, (A), and AMPK (B,C), using immunoblotting. β -actin was used as housekeeping protein. The inhibitor was compound C,

an AMPK activation inhibitor. Different letters (a–d) above the sample groups indicate that the difference between each group is statistically significant ($p < 0.05$) compared to the untreated differentiated control (compared to 0 h in (C)).

3.4. Wnt/ β -Catenin Signaling during Adipogenic Differentiation of hBM-MSCs

The effect of loliolide on the Wnt/ β -catenin pathway was determined by detecting Wnt 10b and β -catenin protein levels in adipo-induced hBM-MSCs (Figure 4). The results show that adipogenic differentiation of hBM-MSCs notably inhibited the levels of Wnt 10b whereas loliolide treatment (10 μ M) increased Wnt 10b levels significantly. Next, the downstream effector of Wnt activation, β -catenin, was evaluated. Adipogenic differentiation decreased the Ser675 phosphorylated levels of β -catenin along with Axin protein, which is a part of the β -catenin degradational complex, indicating that adipogenesis resulted in increased degradation of β -catenin. The results show no changes in Axin levels following loliolide treatment; however, p-(Ser675) β -catenin levels were increased substantially (Figure 4A). The effect of loliolide on stimulating Wnt signaling was also confirmed by immunostaining of Wnt 10b in adipo-induced hBM-MSCs. Fluorescence staining of Wnt 10b protein displayed that loliolide treatment significantly attenuated adipogenesis-induced decrease in Wnt 10b levels (Figure 4B). Further support for the β -catenin activity stimulatory effect of loliolide came from analyzing nuclear and cytosolic fractions of the cells by Western blot. Loliolide treatment decreased the p- β -catenin levels in cytosol while increasing its levels in nuclear fractions (Figure 4C). In addition, decreased PPAR γ levels in nuclear fractions of adipo-induced hBM-MSCs indicated that loliolide treatment suppressed the adipogenic differentiation through enhancement of the Wnt/ β -catenin pathway activation, which resulted in inhibited PPAR γ levels.

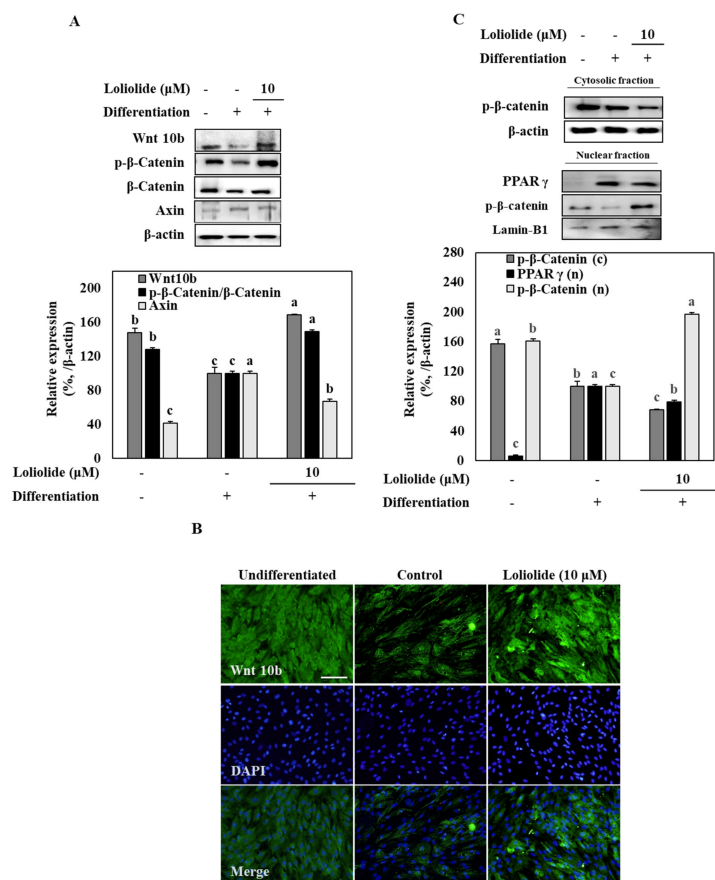


Figure 4. The effect of loliolide treatment on the Wnt/ β -catenin pathway. The hBM-MSCs were differentiated into adipocytes in six-well plates with or without loliolide treatment (10 μ M). One group was left untreated and non-differentiated as

the negative control. The hBM-MSCs at Day 10 of differentiation were used for the analysis of total and phosphorylated (p-) Wnt, β -catenin, and Axin (A) using immunoblotting. β -actin was used as housekeeping protein. The inhibitor was compound C, an AMPK activation inhibitor. Different letters (a-c) above the sample groups indicate that the difference between each group is statistically significant ($p < 0.05$) compared to the untreated differentiated control. (B) Images of fluorescence-stained hBM-MSCs at incubation Day 10 after adipogenesis inducement (except undifferentiated untreated group which was fed growth medium only), stained with FITC conjugated anti-Wnt 10b antibody (green) and DAPI (blue) to highlight the nuclei. Scale bar, 100 μ m. (C) Cell lysates were separated between cytosolic (c) and nuclear (n) fractions, and protein levels of p- β -catenin and PPAR γ were detected using immunoblotting. Lamin-B1 was used as the internal control. Different letters (a-c) above the sample groups indicate that the difference between each group is statistically significant ($p < 0.05$) compared to the untreated differentiated control.

4. Discussion

Excessive adipose tissue, which is one of the easily conformable markers of obesity progression, is mainly a result of uncontrolled formation of new adipocytes. The formation of adipose tissue occurs via increased lipid storage via adipocytes differentiated from mesenchymal stromal cells in either adipose tissue or bone [26]. This uncontrolled formation of new adipocytes is often linked with other diseases such as osteoporosis as an underlying cause or stimulatory factor [27]. The obesity-linked complications and deterioration that affects the behaviors of bone-marrow MSCs are the main cause of several other metabolic syndrome-related complications. Therefore, the current study tested the effects of loliolide on adipogenesis using hBM-MSC models. To the best of our knowledge, this is the first report of loliolide-aided inhibition of adipogenesis in MSCs.

Loliolide has been reported a bioactive phytochemical with various health benefits due to its antioxidant, antitumor, antiaging, and anti-inflammatory properties [17,20]. Although its effect on inhibiting adipogenesis was reported in murine pre-adipocytes, there has been no report of loliolide indicating its effect on differentiation of any type of MSCs. As a part of ongoing research to develop anti-obesity natural products, this study employed hBM-MSCs as the model to screen the effect of loliolide on adipogenesis and provide comparison data on whether loliolide's effect on murine pre-adipocytes could be observed in human MSCs, which are the source of adipose tissue in the human body.

Lipid accumulation as intracellular lipid droplets is a key characteristic of adipocytes and observed during the maturation of adipocytes [28]. Loliolide treatment decreased the lipid accumulation in adipo-induced hBM-MSCs, indicating its inhibitory effect in early stages of adipogenic differentiation or stimulatory effect on lipolysis. To determine whether loliolide inhibits adipogenic differentiation, the PPAR γ pathway was examined. PPAR γ is a well-known and intensely studied transcription factor for adipogenesis along with its upstream effector C/EBP α [29]. Loliolide-treated hBM-MSCs exerted a dose-dependent drop at the levels of mRNA and protein expression for PPAR γ and C/EBP α . Treatment with loliolide also suppressed the expression of SREBP1c, which is an adipocyte-specific gene [30]. These results suggest that loliolide inhibited the adipogenic differentiation with an influence on PPAR γ signaling by modulating early stages of adipogenesis via PPAR γ and C/EBP α expression.

To determine the underlying mechanisms behind the anti-adipogenic effect of loliolide, signaling pathways that regulate PPAR γ activation were analyzed. The AMPK and MAPK signaling pathways are such pathways with vital roles in adipogenesis. MAPK-mediated regulation of adipogenesis is primarily dependent on the cell type, experimental conditions, and extracellular stimuli [24]. Reports have shown that, while ERK phosphorylation may be involved in both stimulation and inhibition of adipogenesis, p38 and JNK phosphorylation is in mostly involved in adipogenesis stimulation [31,32]. Nevertheless, the current results show that adipogenesis in hBM-MSCs came with elevated activation of MAPKs. Loliolide was able to prevent adipogenesis-induced phosphorylation of p38 and JNK but was ineffective against ERK. Although being closely related with MAPK activation, the role of AMPK in adipogenesis is readily reported. It is known that AMPK activation plays

various roles in cellular mechanisms against obesity, diabetes, and metabolic diseases [33]. In addition to its roles in energy and lipid metabolisms, AMPK signaling is involved in adipogenesis by being suppressed concurrently during PPAR γ activation [34]. Inhibiting AMPK activation has been shown to increase the expression of adipogenic markers including PPAR γ . Loliolide treatment attenuated the adipogenic suppression of AMPK phosphorylation in the presence of AMPK inhibitor compound C at the early stages of adipogenesis. Attenuation of AMPK phosphorylation indicated that loliolide suppressed the adipogenesis at the early stages via AMPK/MAPK signaling.

Canonical Wnt/ β -catenin signaling is also involved in adipogenic differentiation of MSCs. Adipogenic stimulation of cells is known to antagonize the Wnt/ β -catenin pathway [35]. Increased degradation of β -catenin is observed along elevated PPAR γ translocation to nucleus, resulting in expression of adipogenic genes. Although Wnt signaling induces stem cells to differentiate into pre-adipocyte to commit adipogenic lineage, it also inhibits the adipocyte maturation of pre-adipocytes [36,37]. Wnt 10b is a Wnt subunit that is expressed in MSCs, and its overexpression was shown to decrease adipogenesis [38]. Phosphorylation of β -catenin at Ser31, Ser41, and Thr47 facilitates its degradation and stimulates the adipogenic differentiation at the early stages of MSCs adipogenic differentiation [39]. However, Ser675 phosphorylated β -catenin via the activities of pKA was reported to induce its nuclear translocation and transcriptional activity [40]. In a previous report, this translocation of β -catenin was suggested to lead to the inhibition of PPAR γ activity as a result of β -catenin-PPAR γ binding [41]. The current results show that loliolide treatment not only elevated the Wnt10b levels in hBM-MSC adipocytes, but also stimulated the nuclear translocation of active β -catenin. Lee et al. [42] showed that loliolide stimulated the dephosphorylation of β -catenin through enhancement of AKT/PKA-mediated phosphorylation in human dermal papilla cells, hence activating Wnt signaling. These results are in agreement with current findings, further supporting the effect of loliolide on Wnt/ β -catenin pathway. Overall, it was suggested that loliolide inhibited the adipogenic differentiation of hBM-MSCs via activation of Wnt/ β -catenin, which resulted in AMPK-mediated suppression of PPAR γ activity.

Although loliolide has been reported to alter the gene expressions to exert its bioactivities, *in vivo* studies showing whether these effects could be observed at the phenotype levels are lacking. To the best of our knowledge, only the antioxidant effect of loliolide was observed in zebrafish models *in vivo* where loliolide reduced the 2,2'-azobis(2-amidinopropane) dihydrochloride-induced lipid peroxidation [43]. This suggested that the changes induced by loliolide at gene level might be present at phenotype level as well. Considering the potential loliolide holds, future studies to explore the effect of loliolide on adipogenesis at transcriptome and epigenome levels via *in vivo* models are urged.

In summary, loliolide was revealed to repress adipogenic differentiation of hBM-MSCs via activating the AMPK and Wnt/ β -catenin signaling which subsequently resulted in suppressed PPAR γ pathway (Figure 5). It was suggested that loliolide is a promising phytochemical with anti-adipogenic properties, although further *in vivo* studies are needed to better evaluate its potential and mechanism of action. Nonetheless, the current study provided important reference for future studies to develop loliolide-centered agents for prevention and treatment of obesity and related complications.

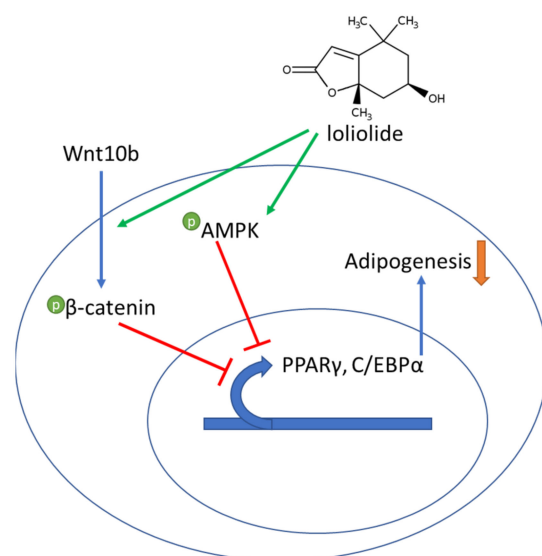


Figure 5. A hypothesis of the mechanism of action of the adipogenesis inhibitory effect of loliolide on adipo-induced hBM-MSCs.

Author Contributions: Conceptualization and methodology, F.K., J.H.O., and Y.S.; validation, formal analysis, and investigation, J.H.O., M.-S.J., and H.K.; resources, Y.S. and C.-S.K.; data curation, F.K., C.-S.K., and Y.S.; writing—original draft preparation, visualization, F.K. and J.H.O.; supervision and project administration, C.-S.K. and Y.S.; and funding acquisition, M.-S.J. and C.-S.K. All authors have read and agreed to the published version of the manuscript.

Funding: This study was supported by a grant from the National Institute of Fisheries Science (R2021062) and the BB21+ Project in 2021.

Institutional Review Board Statement: Not applicable.

Informed Consent Statement: Not applicable.

Data Availability Statement: All data used to support the findings of this study are available from the corresponding author upon reasonable request.

Conflicts of Interest: The authors declare no conflict of interest.

References

- Hill, J.H.; Solt, C.; Foster, M.T. Obesity associated disease risk: The role of inherent differences and location of adipose depots. *Horm. Mol. Biol. Clin. Investig.* **2018**, *33*, 20180012. [[CrossRef](#)] [[PubMed](#)]
- Kang, C.; LeRoith, D.; Gallagher, E.J. Diabetes, obesity, and breast cancer. *Endocrinology* **2018**, *159*, 3801–3812. [[CrossRef](#)] [[PubMed](#)]
- Srivastava, G.; Apovian, C. Future pharmacotherapy for obesity: New anti-obesity drugs on the horizon. *Curr. Obes. Rep.* **2018**, *7*, 147–161. [[CrossRef](#)] [[PubMed](#)]
- Bahmad, H.F.; Daouk, R.; Azar, J.; Sapudom, J.; Teo, J.C.M.; Abou-Kheir, W.; Al-Sayegh, M. Modeling adipogenesis: Current and future perspective. *Cells* **2020**, *9*, 2326. [[CrossRef](#)] [[PubMed](#)]
- Bacakova, L.; Zarubova, J.; Travnickova, M.; Musilkova, J.; Pajorova, J.; Slepicka, P.; Kasalkova, N.S.; Svorcik, V.; Kolska, Z.; Motarjemi, H.; et al. Stem cells: Their source, potency and use in regenerative therapies with focus on adipose-derived stem cells—A review. *Biotechnol. Adv.* **2018**, *36*, 1111–1126. [[CrossRef](#)]
- Fassio, A.; Idolazzi, L.; Rossini, M.; Gatti, D.; Adami, G.; Giollo, A.; Viapiana, O. The obesity paradox and osteoporosis. *Eat. Weight Disord. Stud. Anorexia, Bulim. Obes.* **2018**, *23*, 293–302. [[CrossRef](#)]
- Da Silva, S.V.; Renovato-Martins, M.; Ribeiro-Pereira, C.; Citelli, M.; Barja-Fidalgo, C. Obesity modifies bone marrow microenvironment and directs bone marrow mesenchymal cells to adipogenesis. *Obesity* **2016**, *24*, 2522–2532. [[CrossRef](#)] [[PubMed](#)]
- Hardouin, P.; Rharass, T.; Lucas, S. Bone marrow adipose tissue: To be or not to be a typical adipose tissue? *Front. Endocrinol.* **2016**, *7*, 85. [[CrossRef](#)]
- Lee, J.; Abdeen, A.A.; Tang, X.; Saif, T.A.; Kilian, K.A. Matrix directed adipogenesis and neurogenesis of mesenchymal stem cells derived from adipose tissue and bone marrow. *Acta Biomater.* **2016**, *42*, 46–55. [[CrossRef](#)]

10. Shao, X.; Wang, M.; Wei, X.; Deng, S.; Fu, N.; Peng, Q.; Jiang, Y.; Ye, L.; Xie, J.; Lin, Y. Peroxisome proliferator-activated receptor- γ : Master regulator of adipogenesis and obesity. *Curr. Stem Cell Res. Ther.* **2016**, *11*, 282–289. [[CrossRef](#)]
11. James, A.W. Review of signaling pathways governing MSC osteogenic and adipogenic differentiation. *Scientifica* **2013**, *2013*, 1–17. [[CrossRef](#)] [[PubMed](#)]
12. Takada, I.; Kouzmenko, A.P.; Kato, S. Wnt and PPAR γ signaling in osteoblastogenesis and adipogenesis. *Nat. Rev. Rheumatol.* **2009**, *5*, 442–447. [[CrossRef](#)] [[PubMed](#)]
13. Nuttall, M. Controlling the balance between osteoblastogenesis and adipogenesis and the consequent therapeutic implications. *Curr. Opin. Pharmacol.* **2004**, *4*, 290–294. [[CrossRef](#)]
14. Chen, J.-R.; Lazarenko, O.P.; Wu, X.; Tong, Y.; Blackburn, M.L.; Shankar, K.; Badger, T.M.; Ronis, M.J.J. Obesity reduces bone density associated with activation of PPAR γ and suppression of Wnt/ β -catenin in rapidly growing male rats. *PLoS ONE* **2010**, *5*, e13704. [[CrossRef](#)] [[PubMed](#)]
15. Grabarczyk, M.; Wińska, K.; Mączka, W.; Potaniec, B.; Anioł, M. Loliolide - the most ubiquitous lactone. *Folia Biol. Oecologica* **2015**, *11*, 1–8. [[CrossRef](#)]
16. Yang, X.; Kang, M.C.; Lee, K.W.; Kang, S.M.; Lee, W.W.; Jeon, Y.J. Antioxidant activity and cell protective effect of loliolide isolated from *Sargassum ringgoldianum* subsp. *Coreanum*. *ALGAE* **2011**, *26*, 201–208. [[CrossRef](#)]
17. Chung, C.Y.; Liu, C.H.; Burnouf, T.; Wang, G.H.; Chang, S.P.; Jassey, A.; Tai, C.J.; Tai, C.J.; Huang, C.J.; Richardson, C.D.; et al. Activity-based and fraction-guided analysis of *Phyllanthus urinaria* identifies loliolide as a potent inhibitor of hepatitis C virus entry. *Antivir. Res.* **2016**, *130*, 58–68. [[CrossRef](#)]
18. Lee, H.-G.; Kim, H.-S.; Je, J.-G.; Hwang, J.; Sanjeeva, K.K.A.; Lee, D.-S.; Song, K.-M.; Choi, Y.-S.; Kang, M.-C.; Jeon, Y.-J. Lipid inhibitory effect of (–)-loliolide isolated from *Sargassum horneri* in 3T3-L1 adipocytes: Inhibitory mechanism of adipose-specific proteins. *Mar. Drugs* **2021**, *19*, 96. [[CrossRef](#)]
19. Kim, S.Y.; Lee, J.Y.; Jhin, C.; Shin, J.M.; Kim, M.; Ahn, H.R.; Yoo, G.; Son, Y.J.; Jung, S.H.; Nho, C.W. Reduction of hepatic lipogenesis by loliolide and pinoresinol from *Lysimachia vulgaris* via degrading liver α receptors. *J. Agric. Food Chem.* **2019**, *67*, 12419–12427. [[CrossRef](#)]
20. Kim, H. Isolation and Structure Determination of Matrix Metalloproteinase Inhibitors and Antioxidants from *Ligustrum japonicum fructus*, *Zostera asiatica* and *Artemisia princeps*. Ph.D. Thesis, Korea Maritime and Ocean University, Busan, Korea, 2019.
21. Park, K.E.; Kim, Y.A.; Jung, H.A.; Lee, H.J.; Ahn, J.W.; Lee, B.J.; Seo, Y. Three norisoprenoids from the brown alga *Sargassum thunbergii*. *J. Korean Chem. Soc.* **2004**, *48*, 394–398. [[CrossRef](#)]
22. Karadeniz, F.; Oh, J.H.; Lee, J.I.; Kim, H.; Seo, Y.; Kong, C.S. 6-acetyl-2,2-dimethylchroman-4-one isolated from *Artemisia princeps* suppresses adipogenic differentiation of human bone marrow-derived mesenchymal stromal cells via activation of AMPK. *J. Med. Food* **2020**, *23*, 250–257. [[CrossRef](#)] [[PubMed](#)]
23. Menssen, A.; Haupl, T.; Sittlinger, M.; Delorme, B.; Charbord, P.; Ringe, J. Differential gene expression profiling of human bone marrow-derived mesenchymal stem cells during adipogenic development. *BMC Genom.* **2011**, *12*, 461. [[CrossRef](#)]
24. Bost, F.; Aouadi, M.; Caron, L.; Binetruy, B. The role of MAPKs in adipocyte differentiation and obesity. *Biochimie* **2005**, *87*, 51–56. [[CrossRef](#)]
25. Ahmad, B.; Serpell, C.J.; Fong, I.L.; Wong, E.H. Molecular mechanisms of adipogenesis: The anti-adipogenic role of AMP-activated protein kinase. *Front. Mol. Biosci.* **2020**, *7*, 76. [[CrossRef](#)] [[PubMed](#)]
26. Romanov, Y.A.; Darevskaya, A.N.; Merzlikina, N.V.; Buravkova, L.B. Mesenchymal stem cells from human bone marrow and adipose tissue: Isolation, characterization, and differentiation potentialities. *Bull. Exp. Biol. Med.* **2005**, *140*, 138–143. [[CrossRef](#)]
27. Zhao, L.J.; Jiang, H.; Papisian, C.J.; Maulik, D.; Drees, B.; Hamilton, J.; Deng, H.W. Correlation of obesity and osteoporosis: Effect of fat mass on the determination of osteoporosis. *J. Bone Miner. Res.* **2007**, *23*, 17–29. [[CrossRef](#)] [[PubMed](#)]
28. Fu, Y.; Luo, N.; Klein, R.L.; Garvey, W.T. Adiponectin promotes adipocyte differentiation, insulin sensitivity, and lipid accumulation. *J. Lipid Res.* **2005**, *46*, 1369–1379. [[CrossRef](#)] [[PubMed](#)]
29. Lefterova, M.I.; Zhang, Y.; Steger, D.J.; Schupp, M.; Schug, J.; Cristancho, A.; Feng, D.; Zhuo, D.; Stoeckert, C.J.; Liu, X.S.; et al. PPAR and C/EBP factors orchestrate adipocyte biology via adjacent binding on a genome-wide scale. *Genes Dev.* **2008**, *22*, 2941–2952. [[CrossRef](#)] [[PubMed](#)]
30. Payne, V.A.; Au, W.-S.; Lowe, C.E.; Rahman, S.M.; Friedman, J.E.; O’Rahilly, S.; Rochford, J.J. C/EBP transcription factors regulate SREBP1c gene expression during adipogenesis. *Biochem. J.* **2010**, *425*, 215–224. [[CrossRef](#)] [[PubMed](#)]
31. Cao, D.; Ma, F.; Ouyang, S.; Liu, Z.; Li, Y.; Wu, J. Effects of macrophages and CXCR2 on adipogenic differentiation of bone marrow mesenchymal stem cells. *J. Cell. Physiol.* **2018**, *534*, 9475–9485. [[CrossRef](#)]
32. Tanabe, Y. Inhibition of adipocyte differentiation by mechanical stretching through ERK-mediated downregulation of PPAR2. *J. Cell Sci.* **2004**, *117*, 3605–3614. [[CrossRef](#)]
33. Fogarty, S.; Hardie, D.G. Development of protein kinase activators: AMPK as a target in metabolic disorders and cancer. *Biochim. Biophys. Acta Proteins Proteom.* **2010**, *1804*, 581–591. [[CrossRef](#)] [[PubMed](#)]
34. Lee, W.H.; Kim, S.G. AMPK-dependent metabolic regulation by PPAR agonists. *PPAR Res.* **2010**, *2010*, 549101. [[CrossRef](#)]
35. Prestwich, T.C.; MacDougald, O.A. Wnt/ β -catenin signaling in adipogenesis and metabolism. *Curr. Opin. Cell Biol.* **2007**, *19*, 612–617. [[CrossRef](#)]
36. Ling, L.; Nurcombe, V.; Cool, S.M. Wnt signaling controls the fate of mesenchymal stem cells. *Gene* **2009**, *433*, 1–7. [[CrossRef](#)]

37. Xu, C.; Wang, J.; Zhu, T.; Shen, Y.; Tang, X.; Fang, L.; Xu, Y. Cross-talking between PPAR and WNT signaling and its regulation in mesenchymal stem cell differentiation. *Curr. Stem Cell Res. Ther.* **2016**, *11*, 247–254. [[CrossRef](#)] [[PubMed](#)]
38. Cawthorn, W.P.; Bree, A.J.; Yao, Y.; Du, B.; Hemati, N.; Martinez-Santibañez, G.; MacDougald, O.A. Wnt6, Wnt10a and Wnt10b inhibit adipogenesis and stimulate osteoblastogenesis through a β -catenin-dependent mechanism. *Bone* **2012**, *50*, 477–489. [[CrossRef](#)] [[PubMed](#)]
39. Xu, L.; Song, C.; Ni, M.; Meng, F.; Xie, H.; Li, G. Cellular retinol-binding protein 1 (CRBP-1) regulates osteogenesis and adipogenesis of mesenchymal stem cells through inhibiting RXR α -induced β -catenin degradation. *Int. J. Biochem. Cell Biol.* **2012**, *44*, 612–619. [[CrossRef](#)] [[PubMed](#)]
40. Meng, J.; Ma, X.; Wang, N.; Jia, M.; Bi, L.; Wang, Y.; Li, M.; Zhang, H.; Xue, X.; Hou, Z.; et al. Activation of GLP-1 receptor promotes bone marrow stromal cell osteogenic differentiation through β -catenin. *Stem Cell Rep.* **2016**, *6*, 579–591. [[CrossRef](#)] [[PubMed](#)]
41. Lee, H.; Bae, S.; Kim, K.; Kim, W.; Chung, S.I.; Yoon, Y. β -catenin mediates the anti-adipogenic effect of baicalin. *Biochem. Biophys. Res. Commun.* **2010**, *398*, 741–746. [[CrossRef](#)]
42. Lee, Y.R.; Bae, S.; Kim, J.Y.; Lee, J.; Cho, D.H.; Kim, H.S.; An, I.S.; An, S. Monoterpenoid loliolide regulates hair follicle inductivity of human dermal papilla cells by activating the Akt/ γ -Catenin signaling pathway. *J. Microbiol. Biotechnol.* **2019**, *29*, 1830–1840. [[CrossRef](#)] [[PubMed](#)]
43. Kim, H.-S.; Wang, L.; Fernando, I.P.S.; Je, J.-G.; Ko, S.-C.; Kang, M.C.; Lee, J.M.; Yim, M.J.; Jeon, Y.J.; Lee, D.S. Antioxidant efficacy of (–)-loliolide isolated from *Sargassum horneri* against AAPH-induced oxidative damage in Vero cells and zebrafish models in vivo. *J. Appl. Phycol.* **2020**, *32*, 3341–3348. [[CrossRef](#)]